

DETC2017-67371

ANALYSIS OF DIFFERENTIAL MECHANISMS FOR A ROBOTIC HEAD STABILIZATION SYSTEM

Adam Williams

Robotics and Mechatronics Lab
Mechanical Engineering Dept.
Virginia Tech
Blacksburg, VA 24061
aw13@vt.edu

Wael Saab

Robotics and Mechatronics Lab
Mechanical Engineering Dept.
Virginia Tech
Blacksburg, VA 24061
waelsaab@vt.edu

Pinhas Ben-Tzvi

Robotics and Mechatronics Lab
Mechanical Engineering Dept.
Virginia Tech
Blacksburg, VA 24061
bentzvi@vt.edu

ABSTRACT

This paper presents a robotic system intended to help automate the head and neck stabilization process performed on trauma patients through application of a differential apparatus, a device that distributes an input between multiple output channels. A system to streamline the head stabilization process can save valuable time in a life and death scenario, as well as play a key role in future work on a mobile stretcher robot. This investigation focuses on finding the most suitable device to accommodate multiple possible head positions while maintaining a steady force in order to provide secure motion restriction. After an initial review of current emergency medical services standards, a comparison of potential differential mechanisms is undertaken. Static analysis as well as dynamic modeling is performed in order to determine the most appropriate mechanisms. An initial prototype design incorporating a differential pulley, the most mechanically advantageous mechanism, is then introduced.

1 INTRODUCTION

Traumatic injury can often result in dangerous and even fatal damage to the spinal cord, with 20% of such injuries resulting in fatalities before patients are even admitted to a hospital [1]. In cases that do not result in fatalities, spinal injuries can result in paralysis, chronic pain, and long-term hospitalization. When assisting trauma patients, first responders take extensive precautions to minimize head motion in order to prevent further damage or injury to the spinal cord in the neck (cervical spine).

In the 2002 Guidelines for the Management of Acute Spine and Spinal Cord Injuries, published by the American Association of Neurological Surgeons, the recommended procedure for all cases in which a cervical spinal injury is suspected is to stabilize the patient using “a cervical collar and

supporting blocks” [2]. Figure 1 demonstrates standard neck stabilization and immobilization.

The Emergency Medical Technician (EMT) National Curriculum concurs; recommending a standard procedure should the responding EMTs suspect the patient has suffered a neck injury. The procedure is as follows:

1. The neck should be manually stabilized in-line with the spine.
2. A rigid immobilization device (i.e. cervical collar) should be applied.
3. The head and neck should be stabilized using supporting blocks, sand bags, or similar devices [3].

However, despite the recommendation that cervical collars be applied only when a cervical spine injury is suspected, in common practice rigid collars are often applied to all trauma patients regardless of the presence of a suspected neck injury.

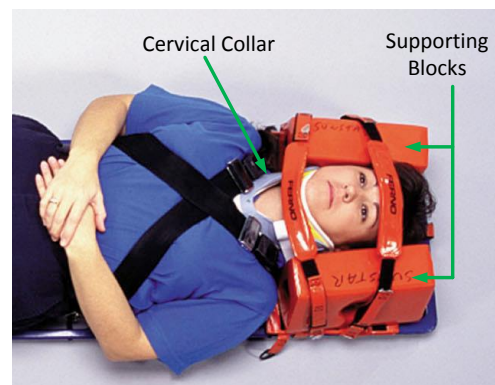


Figure 1. Example of Standard Neck Stabilization and Immobilization [4]

Recent research has shown higher than expected rates of complications associated with unnecessary use of rigid cervical

collars, such as ankylosing spondylitis (an arthritis of the spine), increases in intracranial pressure resulting in head injury, compromised airway management, and delayed resuscitation of patients with penetrating trauma [5]. This has sparked extensive work investigating the benefits and the hazards of the use of such collars [6], [7]. The research has led to new guidelines and procedures for the neck stabilization, calling for reduced and more discretionary use of rigid cervical collars in trauma situations [8], with some suggesting an algorithmic evaluation of the injury severity to determine the necessity of spinal immobilization [9], [10]. Other researchers have questioned the benefits of any immobilization, finding fewer complications in foreign hospitals that do not practice pre-hospital immobilization [11].

This paper will investigate design components for a compliant robotic head stabilization system utilizing supporting blocks. Due to the uncertain benefits of rigid collar application and the requirement of case-by-case evaluation for its use, automated cervical collar application strategies will not be considered in this investigation.

A major design goal for the system will be to have the two supporting blocks driven by a single actuator. Each block will maintain the freedom to reach an asymmetric final position, while applying constant force to hold the head steady without causing discomfort. The allowance of an asymmetric final position will give the device the ability to stabilize the head and neck in the position in which the patient is originally encountered or in the position in which it is manually placed by a trained emergency medical professional. In addition, the asymmetry will help the device to better accommodate patients wearing headgear or helmets. An asymmetric final position is achievable through incorporation of a differential mechanism, which applies a single input to two or more outputs independently. Therefore, the use of this system as designed would result in the patient being protected against further injury from excessive motion of the head, and the potentially injurious effects of unnecessary in-line stabilization could be avoided.

When evaluating the benefits of the system as a standalone device, an important statistic to consider is the mean time for neck stabilization by medical first responders, which was found to be 5.64 min +/- 1.49 min [12]. The incorporation of an automatic head stabilization system into standard first responder equipment could decrease that time, an important benefit in a life-saving scenario. In addition, automatic active stabilization removes the necessity for a medic to manually stabilize the head continuously until a cervical collar is correctly applied when deemed necessary by the medical responders. This would be an especially valuable benefit for two-man first responder teams by making that medic available to do other critical tasks [13].

This paper will analyze the various differential mechanisms in order to determine the design benefits incurred from the use of such mechanisms. To quantify the comparison process, a static analysis similar to that performed by Birglen and Gosselin in [14] will be incorporated. In order to provide analysis for simulation and controller design via force analysis in multiple

operation modes, a dynamic simulation derived through first principles and geometric analysis of the mechanisms is performed. A proposed design for a robotic neck stabilizer will then incorporate the most mechanically advantageous mechanism.

1.1 PRIOR WORK

Few projects have investigated robotic stabilization of the head in rescue situations. A study was conducted by Yim et al. on the use of a foam based stabilization system for a modular rescue robotic system, where a foam gel was sprayed by a robotic module around the patient's head and allowed to set in a cardboard mold [15]. While the foam provided good support, it required a set amount of time to harden around the patient's head. After transport, the foam would often stick to the head of the patient, requiring it to be broken or cut off. While a flexible and customizable support, these drawbacks make foam gel a less than ideal head stabilization method.

The MechaNek is a head stabilization device designed to protect professional race car drivers in crashes [16]. As an upgrade to the Head and Neck Support (HANS) device worn by motorsports drivers, it is intended to clip to a helmet and hook onto the driver's shoulders to provide stability during crashes. Actively actuated cables are connected between the shoulders and head, keeping constant tension but allowing the driver to utilize the full range of motion of their neck. This is an upgrade over the fixed cables of the HANS. By interfacing with the car's onboard computers, the MechaNek will restrain the head when an imminent crash is detected in order to prevent traumatic spine injury. However, this device is solely intended for use as a portion of the protective equipment worn by motorsports drivers and alternative applications have not been described.

1.2 Rescue Robots

Search and rescue is a field in which collaborative robotic systems can provide positive impact, and as such has received more and more attention as technological advancements have increased the capabilities of robotic systems. While there have been many innovative robots built to assist in the search for people in the aftermath of cataclysmic disasters [17]–[21], less work has been devoted to designing robots intended for performing the rescue portion of search and rescue.

Several mobile robotic platforms have been tested in the past as solutions to this problem. The most advanced systems include a stretcher-pulling robot called the Robotic Extraction Vehicle (REX) paired with a larger semi-autonomous transport vehicle called the Robotic Evacuation Vehicle (REV), an anthropomorphic robot called the Battlefield Extraction-Assist Robot (BEAR) that picks up the injured person in its arms and carry them to safety, and an anthropomorphic military version of the robotic nursing assistance robot RONA, called cRoNA [22], [23]. The robots can be seen in Fig. 2 below.

While each design performs well in the primary task of picking up and transporting the injured person, it can be seen from Fig. 2 that each neglects the support of the head during

transport. In the case of the REX/REV system, the single manipulator arm is used by the REX to pull the soldier onto a stretcher it tows [24]. This simple motion has a high possibility of exacerbating any possible spinal injury. On the other hand, BEAR and cRONA transfer the wounded by picking them up in an in-arm carry. While this provides a quick method to lift an injured person, little neck support is provided. In answer to this shortcoming, the patent for BEAR describes the possible deployment of “neck-brace-like equipment” or a “neck splint,” without a specific description of the equipment implementation [25]. The cRONA patent gives the subject similar treatment, explaining that the neck and spine will be protected by the application of a stabilization device which may be inflatable, but again providing little by way of detail or description [26].

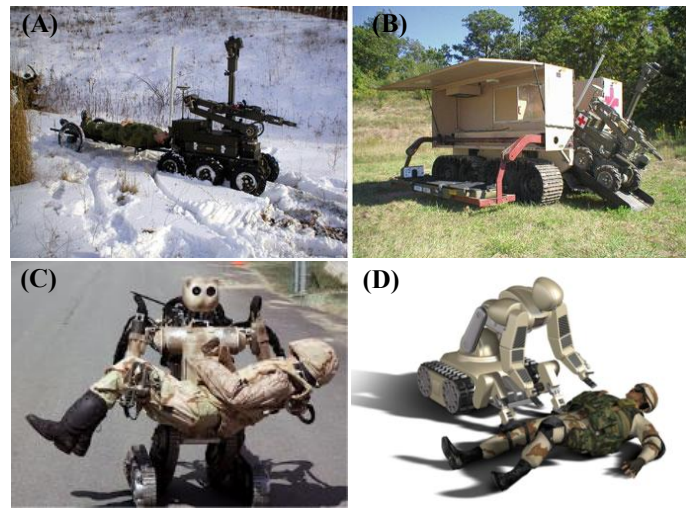


Figure 2. Rescue Robots: (A) REX (B) REX and REV (C) BEAR (D) cRONA

In summary, while the inclusion of neck stabilization methods has been considered in the implementation of robotic rescue platforms, there have been few efforts to design a system intended to perform the stabilization of a person’s head while being rescued.

2 ANALYSIS OF DIFFERENTIAL MECHANISMS

This section begins with review of various types of differential mechanism, followed by qualitative comparisons of possible differential mechanisms as solutions to the stated design task. In addition, the static force calculations are done to compare the mechanisms. The dynamic modeling and simulations are presented. The analyses are compared to determine which mechanism is the most mechanically advantageous for the stated goal of this study.

2.1 Differential Mechanisms

As defined by Hirose in [27], a connected differential mechanism is one in which the dynamic inputs to the mechanism are balanced between multiple “ports,” or degrees of freedom (DOF). As seen in [15] and [19], commonly

encountered examples are shown in Figure 3, including a fluid filled t-pipe, a sliding pulley, a sliding seesaw, and variations of gear-based systems. An easily recognizable differential mechanism is the bevel gear differential found on the drive axle of an automobile. The most common usage of these devices in robotics is in underactuated robotic hands, prosthetics and exoskeletons; sliding pulleys are used in [29]–[31], differential levers in [32]–[34], and a planetary gear differential in [35].

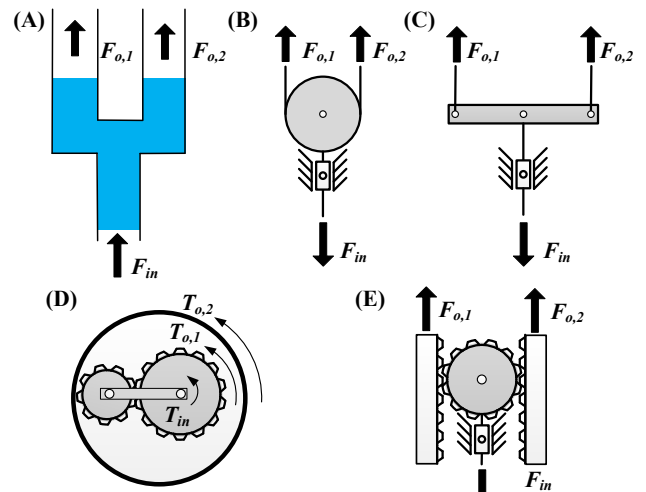


Figure 3. Types of Differential Mechanisms: (A) Fluid T-pipe (B) Sliding Pulley (C) Sliding Seesaw (D) Planetary Gear Differential (E) Rack and Pinion Differential

The driving motivation behind the proliferation of differential mechanisms in robotic hands is the grip adaptability afforded by differential mechanisms, both in terms of compliant finger position and in grip force distribution [36]. In addition, multiple differential mechanisms can be operated in serial and parallel combinations, granting greater flexibility of grip and a closer approximation to experimentally recorded common grip postures, sometimes referred to as synergies [37]. Through application of different versions of differential mechanisms, the input forces and/or displacements can be distributed equally throughout the output channels, such as in [30] and [31], or may be preferentially distributed by selectively varying the geometry of the mechanism such as in [33] and [34]. The non-uniform distribution is often due to the design goal of attributing greater grip force to the thumb in comparison to the force at each of the four remaining fingers.

Furthermore, the ability to couple multiple DOF to a single actuation point greatly reduces the required actuation density for the design. This is of considerable advantage when creating a small form factor device that contains many DOF. As mentioned previously, prior work concerning static force analysis of single and cascading differential devices as well as the desired cable configuration for differential planar manipulators has been conducted by Birglen and Gosselin, Baril et al., and Khakpour et al. in [14], [38], [39]. While similar equilibrium force analysis will be conducted here, additional

investigation was required in order to demonstrate the benefits of the respective mechanisms necessary to choose the most advantageous configuration for the robotic head stabilization system.

For the stated goals of this device, several differential mechanisms can be immediately discarded from consideration. The fluid pipe configuration is undesirable due to the required inclusion of a compressor or pump as well as the risk of leaks. In addition, the gear-based systems necessitate adequate lubrication and require precision manufacturing, increasing the cost to incorporate them into a design. The remaining mechanical devices, the sliding pulley and seesaw, are excellent prospective components. Both combine simplicity of fabrication with similar actuation requirements, leading to analogous static and dynamic data for a straightforward performance comparison. Therefore, these two mechanisms will be the focus of the following analyses.

2.2 Pulley Static Analysis

A free-body diagram of a sliding pulley with diameter R can be seen in Fig. 4. In the system, the pulley would be mounted on a prismatic joint at its center revolute joint, allowing it to translate in both the positive and negative y -direction. The force F_{in} is then applied to the pulley center, creating the resultant output forces $F_{o,1}$ and $F_{o,2}$. These two output forces are equal to the tension forces in the cables. Due to the rotation θ of the pulley to balance the moments applied, the cable angles α_1 and α_2 with respect to the horizontal axis remain constant values.

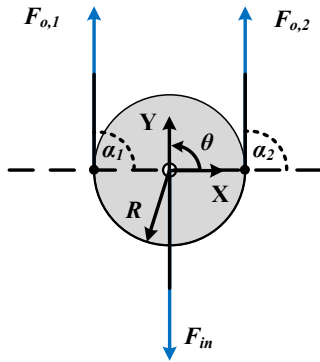


Figure 4. Sliding Pulley Free-Body Diagram

When in equilibrium, the forces on the mechanism can be determined by moment and force balance. The relation between the output forces and the input forces can then be calculated giving Eq. (1) and Eq. (2).

$$F_{o,1} = \frac{F_{o,2} \sin \alpha_2}{\sin \alpha_1} \quad (1)$$

$$F_{o,2} = \frac{-F_{in}}{2 \sin \alpha_2} \quad (2)$$

The force relations show that the output forces are inversely proportional to the initial angle α_i . It can also be seen that if $\alpha_1 = \alpha_2$, the two forces will always be equal in equilibrium. When $\alpha_1 = \alpha_2 = \pi/2$, the two output forces will both be $-F_{in}/2$. While an initial angle less than $\pi/2$ would result in greater tension forces, the angles would then be proportional to the varying y -displacement of the pulley as the geometry of the system changes. To avoid this, in further analyses of the sliding pulley $\alpha_1 = \alpha_2 = \pi/2$ is chosen to be the initial angle.

2.3 Seesaw Static Analysis

Free-body diagrams for the sliding seesaw of length $2L$ are shown Fig. 5 below, with the pulley at its initial state (A) and after translation and rotation due to asymmetric contact with the head (B). The beam possesses a revolute joint at its center, which would in turn be mounted on a prismatic joint to facilitate translation of the seesaw in the y -direction. An input force F_{in} is applied in the negative y -direction along the prismatic joint. The device will thus transfer its force and inputs to the two output forces $F_{o,1}$ and $F_{o,2}$. Should one block contact the head before the other, the seesaw will rotate about its central revolute joint by an angle θ until equilibrium is achieved. For the two cables, the angle from the vertical is denoted by γ_1 and γ_2 .

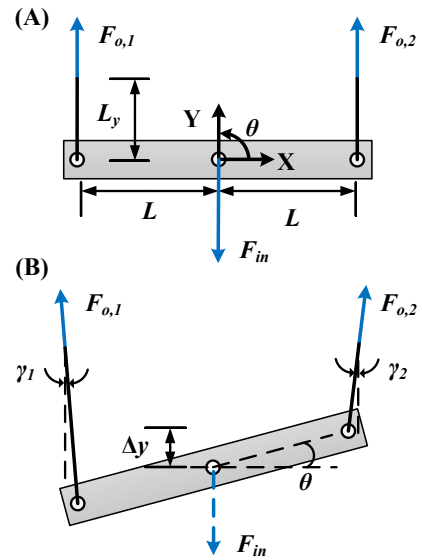


Figure 5. Sliding Seesaw Free-Body Diagram: (A) Initial Position (B) Position Post Rotation and Translation

The angles γ_1 and γ_2 can be calculated using Eq. (3) and Eq. (4), respectively

$$\tan \gamma_1 = \frac{L - L \cos \theta}{L_y + \Delta y + L \sin \theta} \quad (3)$$

$$\tan \gamma_2 = \frac{L - L \cos \theta}{L_y + \Delta y - L \sin \theta} \quad (4)$$

where L_y is the initial vertical cable length and Δy is the vertical displacement of the seesaw along the prismatic joint.

In combination with force and moment balance on the mechanism, Eq. (3) and Eq. (4) can be utilized to give the individual force relations in Eq. (5) and Eq. (6)

$$F_{o,1} = \frac{F_{o,2} \cos \gamma_2}{\cos \gamma_1} \quad (5)$$

$$F_{o,2} = \frac{F_{in}}{2 \cos \gamma_2} \quad (6)$$

It can thus be observed that the seesaw's two force outputs vary independently with θ due to the asymmetry of γ_1 and γ_2 . Again, the redirection pulleys will be placed directly above the beam's cable connection points in order to avoid a dynamically varying initial angle offset.

2.4 Pulley Dynamic Analysis

For the pulley system, the equations relating the motion of the pulley to the forces applied can be found through a geometric analysis of the system. The pulley output cables are wrapped around redirection pulleys to transfer the vertical translation of the sliding pulley to horizontal translation of the supporting blocks. Frictionless rotation with no slip is assumed in all three pulleys. In order to detail the motion that occurs once the right supporting block has made contact with the asymmetrically located head of the patient, the corresponding cable will be treated as if it terminates at a fixed point. The spring component due to the block's compliant foam composition is assumed to be trivial.

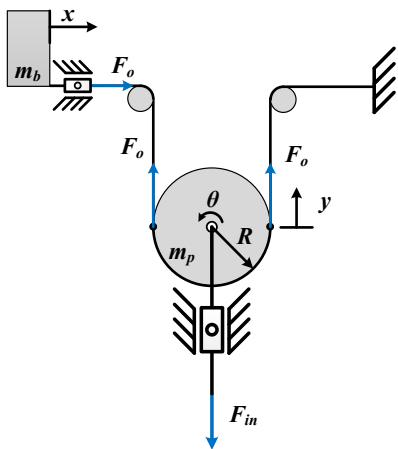


Figure 6. Fixed Cable Sliding Pulley Diagram

A diagram showing the resultant system is shown in Fig. 6, where y is the vertical distance from the pulley starting point, and x is the horizontal distance from the unfixed block's original position. As stated previously, the initial angles between the output cables and the horizontal axis are assumed

to both be $\pi/2$. Due to this symmetry, the two output forces will always be equal, and are represented by F_o .

The cable from one block to the other is observed to be of constant length. By differentiating the sum of the components with respect to time, the relation between \ddot{y} and \ddot{x} is found to be $\ddot{x} = -\ddot{y}/2$. Application of this relation along with force summation at the pulley and block results in Eq. (7), representing the vertical acceleration and Eq. (8) representing the cable tension.

$$\ddot{y} = \frac{F_{in}}{4m_b + m_p} \quad (7)$$

$$F_o = \frac{-F_{in}}{2 + m_p/2m_b} \quad (8)$$

where m_b is the mass of the supporting block and m_p is the mass of the pulley. Note that F_o is independent of the system's motion in this case. The fixed-point assumption holds so long as the tension force F_o is less than the static friction force at the patients head, $m_h g \mu_s$, where m_h is the mass of the head, g is gravitational acceleration, and μ_s is the static friction coefficient.

In addition, the angular acceleration of the pulley is found through the relation between tangential and angular acceleration, $\ddot{y} = R\ddot{\theta}$. Utilizing this and the above equations, a dynamic model of the system was written in MATLAB. Fig. 7 depicts the behavior of the system when the mass of the pulley, m_p , is 0.1 kg, the radius of the pulley, R , is 0.1 m, the mass of the supporting block, m_b , is 2 kg, and a constant force, F_{in} , of 0.5 N is applied in the negative y direction.

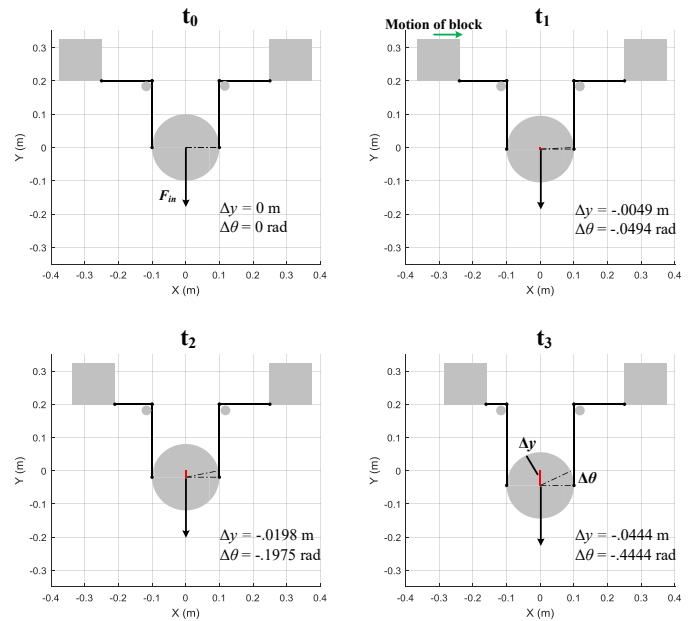


Figure 7. Dynamic Model of Sliding Pulley System

As depicted in Fig. 6, the support block on the right remains fixed. The induced rotation in the pulley due to the fixed constraint results in the translation of the left block in the positive x direction. The dynamic model reinforces the expected motion of the system.

2.5 Seesaw Dynamic Analysis

Applying similar geometric analysis methods as in the previous section lead to the equations describing the motion of the seesaw after the supporting block on the right has contacted the patient's head. Again, the block on the right is replaced with fixed cable termination, the pulleys' motion is assumed to be frictionless, and the spring component in the block in contact with the head due to the block's compliant foam composition is assumed to be trivial.

The resultant system is seen in Fig. 8. The cable tension of the cable connected to the moving block is denoted by $F_{o,1}$, while that of the fixed cable is $F_{o,2}$. As with the pulley, the input force is represented by F_{in} . In the diagram, y is the vertical distance from the initial seesaw position, and x is the horizontal distance from the moving block's original position. The seesaw mass is represented as m_s and the supporting block mass is m_b . The seesaw is depicted a short time after the right block has contacted the person's head in order to demonstrate a small degree of rotation and the corresponding configuration.

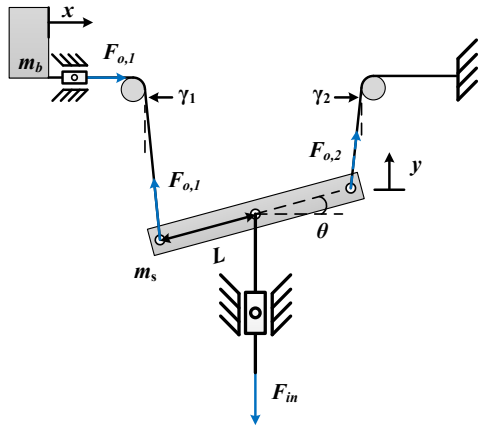


Figure 8. Fixed Cable Sliding Seesaw Diagram

The cable from the connection point on the left side of the seesaw to the supporting block is a fixed length. By differentiating the sum of the components of the cable, the relation between linear and rotational acceleration is found to be $\ddot{x} = -\ddot{y} - \ddot{\theta}L \cos \theta + \dot{\theta}^2 \cos \theta$. This can be combined with the results of the force balance of the beam and block to derive the equations of motion. The vertical acceleration is calculated by Eq. (9) and the rotational in Eq. (10). In order to linearize the equations, small angle approximations were applied for appropriate instances of γ_1 and γ_2 .

$$\ddot{y} = \frac{-F_{in} + F_{o,1}(1 + \gamma_1/\gamma_2)}{m_s} \quad (9)$$

$$\ddot{\theta} = \frac{-F_{in} + F_{o,1}(1 + \gamma_1/\gamma_2)}{Lm_s \cos \theta} + \dot{\theta} \tan \theta^2 \quad (10)$$

The tension forces $F_{o,1}$ and $F_{o,2}$ can be calculated with Eq. (11) and Eq. (12), respectively, through the differentiation of the relation between the static cable length of the fixed side and the displacement of the seesaw center, y .

$$F_{o,1} = \frac{F_{in}\gamma_2}{m_b(m_s - 1)(\gamma_1 + \gamma_2) + \gamma_2 m_b} \quad (11)$$

$$F_{o,2} = F_{o,1} \frac{\gamma_1}{\gamma_2} \quad (12)$$

As with the pulley, the fixed-point assumption holds so long as the tension force $F_{o,1}$ is less than the static friction force applied to the patient's head, $m_h g \mu_s$, where m_h is the mass of the head, g is gravitational acceleration, and μ_s is the static friction coefficient.

Using the above equations, a dynamic model of the system was created in MATLAB. The results of a simulated system are shown in Fig. 9, where the mass of the pulley m_s is 0.1 kg, the mass of the block m_b is 2 kg, the pulley half-length L is 0.1 m, and the applied force F_{in} is 0.5 N in the negative y direction.

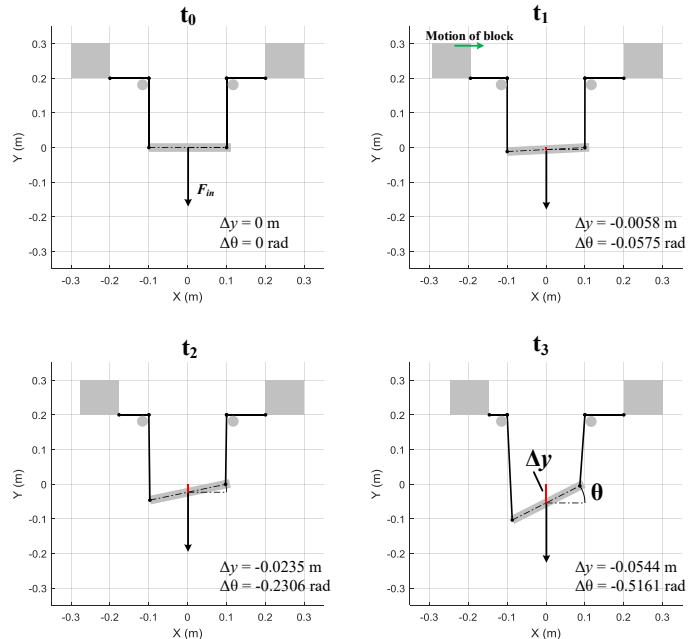


Figure 9. Dynamic Model of Sliding Seesaw System

In the results above, the right block remains statically fixed, as shown in Fig. 8. When a downward force is applied, the cable constraint on the right side induces a counter-clockwise rotation. The rotational motion and the vertical displacement result in the horizontal translation of the left

block. The results of the dynamic model correspond to the expected behavior of the system.

3 DESIGN ANALYSIS CONCLUSIONS AND APPLICATION OF SYSTEM

Several conclusions on the merits of the respective differential mechanisms can be reached through consideration of the results of the prior analyses. Due to the inherent rotation in order to balance the applied moments, the output forces of the pulley are independent of its angle of rotation, θ . In contrast, the seesaw's forces vary with the change in angle γ_1 and γ_2 , which are in turn a function of the angle of rotation. In addition, the seesaw can allow for a maximum misalignment of $2L\sin\theta_{max}$, where θ_{max} is the angle of rotation at which the seesaw is in line with the fixed cable and is a function of the vertical length of the cables as well as the length of the seesaw. Due to this constraint, the seesaw must be sized to have a length proportional to the desired misalignment. In contrast, the amount of misalignment allowed by the pulley is limited only by the total length of the cable. Thus, a much smaller pulley can provide the same degree of compliance as a large seesaw.

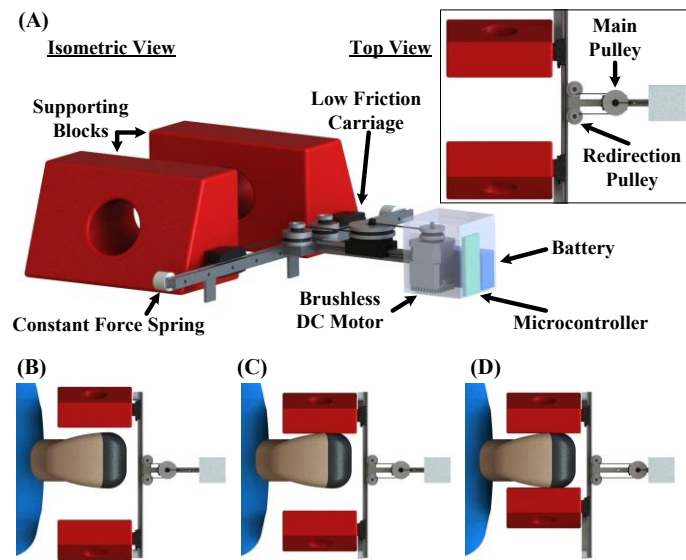


Figure 10. (A) Robotic Head Stabilization System with Inset Top View (B)-(D) System Operation with an Asymmetric Head Location

In summary, it can be concluded that for the purposes of a compliant head support device the most advantageous differential mechanism is a sliding pulley. The sliding pulley will translate along a low friction linear motion carriage mounted on a lightweight aluminum track. The supporting blocks will also be mounted on low friction carriages that translate on an aluminum track perpendicular to that of the sliding pulley. Additionally, the supporting blocks will have small rollers on their base to help facilitate sliding when being translated. A system schematic and an example of its operation

with an asymmetric head location can be seen Fig. 10 above. This configuration has been chosen in order to provide a clear view of the system operation from an overhead view, however future work will involve the optimization of the configuration with an emphasis on compactness and portability.

The redirection pulleys can be optimized to reduce the required range of motion for the sliding pulley. Instead of a single pulley, a two-tiered dual-diameter pulley can be used. The cable on the smaller diameter will be connected to the sliding pulley, while the larger diameter will be connected to the blocks. This applies a gear reduction proportional to the ratio of radii, $n = R_1/R_2$, so that at the cost of increased input force, the linear motion of the sliding pulley is multiplied by a factor of n when redirected to the supporting blocks. In order for the blocks to return to their starting location, constant force springs will be connected to the blocks' roller carriages and to the end of the track. This low force will be easily overcome by the motor, but when the system is put into reverse the force will provide enough tension to pull the blocks back to their original position. An actuation unit containing the motor and controller will be mounted behind the pulley.

A proof-of-concept prototype can be seen in Fig. 11(A) below. A linear actuator is used in this iteration to facilitate the implementation of an extension spring in series with the actuation, creating a series elastic actuator [40]. In order to monitor the force applied to the patient's head without having to directly apply a force sensor array to each block, the SEA will be used to apply the input force and provide force feedback. In Fig. 11 (B)-(D), the actuator is operated directly and the differential pulley demonstrates that it allows for an asymmetrical head location while providing a stabilizing force.

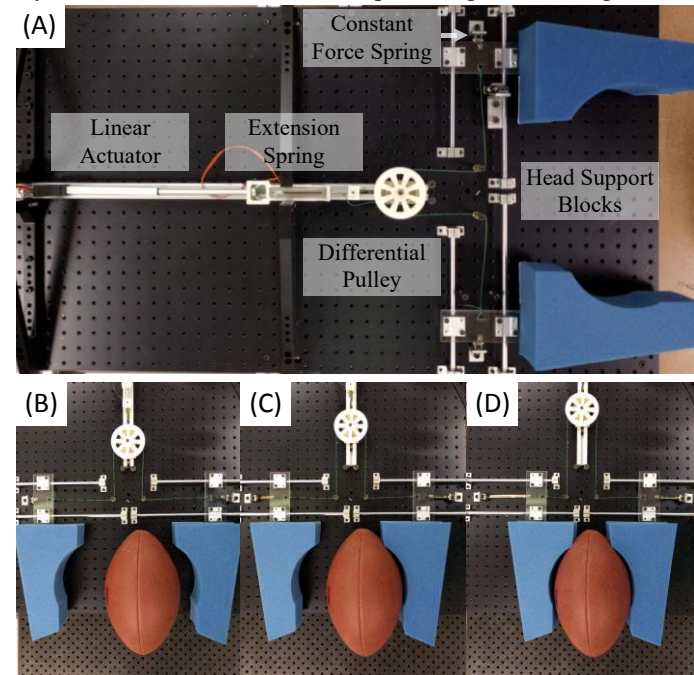


Figure 11. (A) Proof-of-Concept Prototype (B)-(D) System Operation with an Asymmetric Head Location

As mentioned previously, the head stabilization system is intended to function both as a standalone device and as a subsystem on a mobile stretcher robot. In standalone form, the device would be portable, allowing a medical responder to bring it to the location of the injured person. If the medic deems it necessary, he or she could align the patient's head in a more advantageous position. Then the system would be activated and the supporting blocks would gently make contact with the patient's head, holding it in place with constant force.

Additionally, the device can serve as a subsystem for a larger mobile stretcher robot. A semi-autonomous robotic platform designed to transport an incapacitated injured person to safety needs to ensure that no further harm is done and existing injuries are not exacerbated. Therefore, ensuring the person's head and neck are securely supported is a crucial task for such a system. A potential way in which the head stabilization device could be incorporated would be to mount it on the stretcher bed of a robot such as REX, where the system secures the head of the injured person after the robot pulls the person onboard. Another potential method of application would be to put a portable head stabilization system on board a robot such as BEAR or cRONA, which could then place the device at the injured person's head much like a medic would. Once the head is secured, the injured person could be lifted and carried along with the supporting system.

4 CONCLUSION AND FUTURE WORK

This paper presented a comparative investigation of several differential mechanisms, including static and dynamic analyses. Simulations were generated to confirm the desired action of the mechanisms under conditions requiring differential behavior. The results of the analyses led to incorporating a sliding differential pulley into the head stabilization device design.

Future work on the robotic head stabilization system first requires an optimization of the orientation of the sliding pulley block and the actuation unit in order to improve the portability of the system. In addition, further research on the electrical and control components of the system is required. Impedance and force control methods will be also studied in order to provide accurate and precise force control for the system [41].

ACKNOWLEDGMENTS

This work is supported by the US Army Medical Research and Materiel Command under Contract No. W81XWH-16-C-0062. The views, opinions, and/or findings contained in this report are those of the authors and should not be construed as an official Department of the Army position, policy, or decision unless so designated by other documentation.

The authors would like to thank Bijo Sebastian for his work on the geometric analysis of the mechanisms investigated in this paper.

REFERENCES

[1] M. Bernhard, A. Gries, P. Kremer, and B. W. Bottiger, "Spinal

cord injury (SCI) - Prehospital management," *Resuscitation*, vol. 66, no. 2, pp. 127–139, 2005.

[2] M. N. Hadley *et al.*, "Guidelines for the management of acute cervical spine and spinal cord injuries.," *Clin. Neurosurg.*, vol. 49, pp. 407–98, 2002.

[3] D. J. Samuels, H. Bock, K. Mauli, and W. Stoy, *Emergency Medical Technician-Basic: National Standard Curriculum*. 1992.

[4] D. E.-P. Limmer, M. O'Keefe, H. Grant, B. Murray, D. Bergeron, and E. Dickinson, *Emergency Care*, 11th ed. 2008.

[5] R. A. Connell, C. A. Graham, and P. T. Munro, "Is spinal immobilisation necessary for all patients sustaining isolated penetrating trauma?," *Injury*, vol. 34, no. 12, pp. 912–914, 2003.

[6] S. Abram and C. Bulstrode, "Routine spinal immobilization in trauma patients: What are the advantages and disadvantages?," *Surgeon*, vol. 8, no. 4, pp. 218–222, 2010.

[7] T. Sundström, H. Asbjørnsen, S. Habiba, G. A. Sunde, and K. Wester, "Prehospital use of cervical collars in trauma patients: a critical review.," *J. Neurotrauma*, vol. 31, no. 6, pp. 531–40, 2014.

[8] M. N. Hadley *et al.*, "Updated Guidelines for the Management of Acute Cervical Spine and Spinal Cord Injury.," *Neurosurgery*, vol. 72 Suppl 2, no. 3, Mar. 2013.

[9] C. Vaillancourt *et al.*, "The Out-of-Hospital Validation of the Canadian C-Spine Rule by Paramedics," *Ann. Emerg. Med.*, vol. 54, no. 5, pp. 663–671, 2009.

[10] M. Kreinest, B. Gliwitzky, S. Schüler, P. A. Grütznert, and M. Münzberg, "Development of a New Emergency Medicine Spinal Immobilization Protocol for Trauma Patients and a Test of Applicability by German Emergency Care Providers," *Scand. J. Trauma. Resusc. Emerg. Med.*, vol. 24, no. 1, 2016.

[11] M. Hauswald, G. Ong, D. Tandberg, and Z. Omar, "Out-of-hospital spinal immobilization: its effect on neurologic injury.," *Acad. Emerg. Med.*, vol. 5, no. 3, pp. 214–219, 1998.

[12] L. E. Stuke, P. T. Pons, J. S. Guy, W. P. Chapleau, F. K. Butler, and N. E. McSwain, "Prehospital spine immobilization for penetrating trauma-review and recommendations from the prehospital trauma life support executive committee.," *J. Trauma*, vol. 71, no. 3, pp. 763–770, 2011.

[13] D. Jaslow M.D, "Best Practices: Myths and Realities of Spinal Immobilization," *EMSWorld*, 2006. [Online]. Available: <http://www.emsworld.com/article/10322876/best-practices-myths-and-realities-of-spinal-immobilization>. [Accessed: 16-Jan-2017].

[14] L. Birglen and C. Gosselin, "Force Analysis of Connected Differential Mechanisms: Application to Grasping," *Int. J. Rob. Res.*, vol. 25, no. 10, pp. 1033–1046, Oct. 2006.

[15] M. Yim and J. LaCharoen, "Towards small robot aided victim manipulation," *J. Intell. Robot. Syst. Theory Appl.*, vol. 64, no. 1, pp. 119–139, 2011.

[16] M. Gallagher, K. Li, A. Terraciano, B. Banisadr, M. Maltese, and A. Jackson, "MechaNek." [Online]. Available: <http://www.mechanek.com/>. [Accessed: 30-Jan-2017].

[17] P. Ben-Tzvi, "Experimental validation and field performance metrics of a hybrid mobile robot mechanism," *J. F. Robot.*, vol. 27, no. 3, pp. 250–267, 2010.

[18] P. Ben-Tzvi, A. A. Goldenberg, and J. W. Zu, "Design and Analysis of a Hybrid Mobile Robot Mechanism With Compounded Locomotion and Manipulation Capability," *J.*

- Mech. Des.*, vol. 130, no. 7, p. 72302, 2008.
- [19] P. Ben-Tzvi, A. A. Goldenberg, and J. W. Zu, "Articulated hybrid mobile robot mechanism with compounded mobility and manipulation and on-board wireless sensor/actuator control interfaces," *Mechatronics*, vol. 20, no. 6, pp. 627–639, 2010.
- [20] P. M. Moubarak, P. Ben-Tzvi, and Z. Ma, "Mobile Robotic Platform for Autonomous Navigation and Dexterous Manipulation in Unstructured Environments," *ASME Int. Mech. Eng. Congr. Expo.*, pp. 1–8, 2010.
- [21] W. Saab and P. Ben-Tzvi, "A Genderless Coupling Mechanism with 6-DOF Misalignment Capability for Modular Self-Reconfigurable Robots," *J. Mech. Robot.*, vol. 8, no. c, pp. 1–9, 2016.
- [22] A. C. Yoo, G. R. Gilbert, and T. J. Broderick, "Military Robotic Combat Casualty Extraction and Care," in *Surgical Robotics*, Boston, MA: Springer US, 2011, pp. 13–32.
- [23] Hstar Technologies, "HStar Technologies - cRoNA Combat Casualty Extraction and First Responder Robot," 2012. [Online]. Available: <http://www.hstartech.com/index.php/crona.html>.
- [24] R. Watts, P. Rowe, and G. Gilbert, "TATRC and TARDEC Collaborative Robots Program," 2004.
- [25] D. Theobald, "Mobile Extraction-Assist Robot," US Patent 7,719,222 B2, 2010.
- [26] J. Hu and Y.-J. Lim, "Robotic First Responder System and Method," US Patent 20140150806 A1, 2014.
- [27] S. Hirose, "Connected Differential Mechanism and its Applications," in *Proceedings of 1985 Int. Conf. on Advanced Robotics*, 1985, pp. 319–325.
- [28] K. Xu, H. Liu, Zenghui Liu, Y. Du, and X. Zhu, "A single-actuator prosthetic hand using a continuum differential mechanism," in *2015 IEEE Int. Conf. on Robotics and Automation (ICRA)*, 2015, pp. 6547–6462.
- [29] J. T. Belter and A. M. Dollar, "Novel differential mechanism enabling two DOF from a single actuator: Application to a prosthetic hand," in *2013 IEEE 13th Int. Conf. on Rehabilitation Robotics (ICORR)*, 2013, pp. 1–6.
- [30] M. Baril, T. Laliberté, C. Gosselin, and F. Routhier, "On the Design of a Mechanically Programmable Underactuated Anthropomorphic Prosthetic Gripper," *J. Mech. Des.*, vol. 135, no. 12, p. 121008 1-12, 2013.
- [31] G. P. Kontoudis, M. V. Liarokapis, A. G. Zisimatos, C. I. Mavrogiannis, and K. J. Kyriakopoulos, "Open-source, anthropomorphic, underactuated robot hands with a selectively lockable differential mechanism: Towards affordable prostheses," *IEEE Int. Conf. Intell. Robot. Syst.*, vol. 2015–Decem, pp. 5857–5862, 2015.
- [32] M. Rakić, "Multifingered robot hand with selfadaptability," *Robot. Comput. Integr. Manuf.*, vol. 5, no. 2–3, pp. 269–276, 1989.
- [33] R. M. Crowder, "An anthropomorphic robotic end effector," *Rob. Auton. Syst.*, vol. 7, no. 4, pp. 253–268, 1991.
- [34] Y. Kamikawa and T. Maeno, "Underactuated five-finger prosthetic hand inspired by grasping force distribution of humans," in *2008 IEEE/RSJ Int. Conf. on Intelligent Robots and Systems*, 2008, pp. 717–722.
- [35] T. Laliberté and C. Gosselin, "Actuation System for Highly Underactuated Gripping System," US Patent 6,505,870 B1, 2003.
- [36] L. Birglen, T. Laliberté, and C. Gosselin, "Underactuated Robotic Hands," in *Springer Tracts in Advanced Robotics*, 2008, pp. 33–60.
- [37] C. Y. Brown and H. H. Asada, "Inter-finger coordination and postural synergies in robot hands via mechanical implementation of principal components analysis," *IEEE Int. Conf. Intell. Robot. Syst.*, pp. 2877–2882, 2007.
- [38] M. Baril, T. Laliberté, F. Guay, and C. Gosselin, "Static analysis of single-input/multiple-output tendon-driven underactuated mechanisms for robotic hands," in *ASME 2010 Int. Design Engineering Technical Conf. and Computers and Information in Engineering Conf., IDETC/CIE2010*, 2010, vol. 2, pp. 155–164.
- [39] H. Khakpour, L. Birglen, and S. A. Tahan, "Synthesis of differentially driven planar cable parallel manipulators," *IEEE Trans. Robot.*, vol. 30, no. 3, pp. 619–630, 2014.
- [40] G. A. Pratt and M. M. Williamson, "Series elastic actuators," *IEEE/RSJ Int. Conf. Intell. Robot. Syst. 'Human Robot Interact. Coop. Robot.*, vol. 1, no. 1524, pp. 399–406, 1995.
- [41] N. Hogan, "Impedance Control: An Approach to Manipulation: Part I—Theory," *J. Dyn. Syst. Meas. Control*, vol. 107, no. 1, pp. 1–7, 1985.